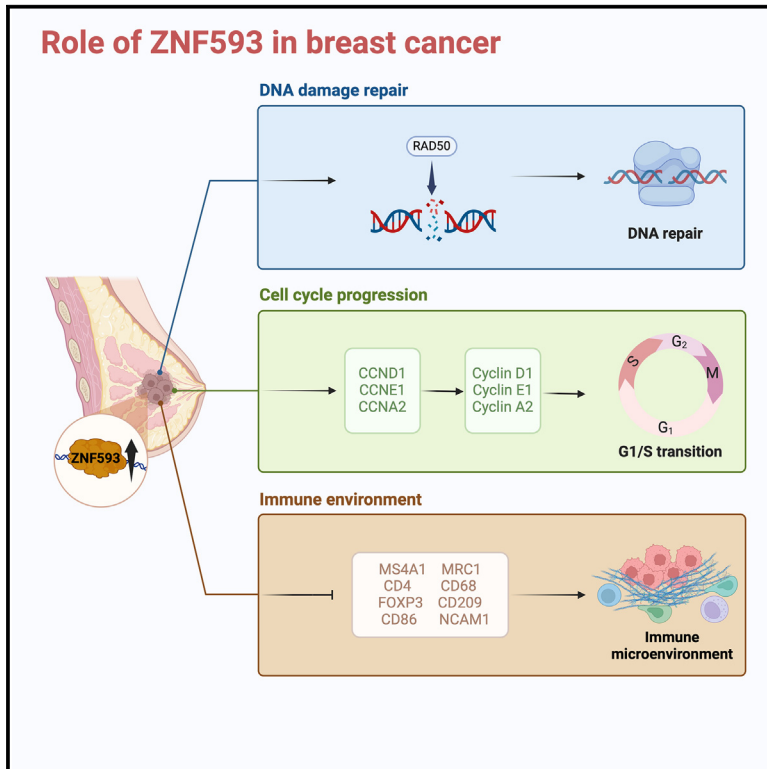


Zinc finger protein 593 promotes breast cancer development by ensuring DNA damage repair and cell-cycle progression

Graphical abstract



Authors

Yingfan Zhang, Xiaowen Tang, Chenxin Wang, ..., Xiang Li, Litong Yao, Yingying Xu

Correspondence

lixiangcmu@163.com (X.L.), ylt_cmu@163.com (L.Y.), xuyingying@cmu.edu.cn (Y.X.)

In brief

Biological sciences; Biochemistry; Protein; Cancer

Highlights

- ZNF593 is highly expressed in breast cancer and correlates with poor prognosis
- ZNF593 is associated with the development and drug resistance of breast cancer
- ZNF593 influences DNA repair and cell-cycle regulation to foster tumor growth



Article

Zinc finger protein 593 promotes breast cancer development by ensuring DNA damage repair and cell-cycle progression

Yingfan Zhang,^{1,4} Xiaowen Tang,^{1,4} Chenxin Wang,¹ Mozhi Wang,¹ Meng Li,² Xiang Li,^{3,*} Litong Yao,^{1,*} and Yingying Xu^{1,5,*}

¹Department of Breast Surgery, the First Hospital of China Medical University, Shenyang, Liaoning, China

²General Surgery Department, Dandong Central Hospital, China Medical University, Dandong, Liaoning, China

³Department of Ultrasound, the First Hospital of China Medical University, Shenyang, Liaoning, China

⁴These authors contributed equally

⁵Lead contact

*Correspondence: lixiangcmu@163.com (X.L.), yit_cmu@163.com (L.Y.), xuyingying@cmu.edu.cn (Y.X.)

<https://doi.org/10.1016/j.isci.2024.111513>

SUMMARY

Breast cancer, a common malignancy and top cause of female cancer deaths globally, urgently requires new biomarkers and insights into its progression and chemoresistance. In this study, we identify ZNF593, a member of the zinc finger protein family, as an understudied oncogene in breast cancer. ZNF593 is significantly upregulated in breast cancer tissues compared to adjacent normal tissues, which is linked to poor prognosis and advanced clinicopathological features. *In vitro* experiments demonstrate that ZNF593 enhances the proliferation and migration capabilities of breast cancer cells. Comprehensive analyses reveal that ZNF593 is associated with DNA damage repair, cell-cycle regulation, and immunity-related pathways. Mechanistically, ZNF593 protects DNA repair and influences sensitivity to the associated chemotherapy. Furthermore, ZNF593 modulates CCND1, CCNE1, and CCNA2, genes encoding cyclins that facilitate the G1/S transition, resulting in cell-cycle progression. Collectively, our findings identify ZNF593 as a potential therapeutic target for breast cancer, affecting progression and chemoresistance.

INTRODUCTION

Breast cancer is the most common cancer among women worldwide and has become the leading cause of cancer-related mortality in most countries in 2024.¹ About a quarter of women with cancer worldwide have breast cancer, whereas about one in six cancer deaths in women worldwide are caused by breast cancer.² The current treatment options for breast cancer include surgery, radiation therapy, chemotherapy, endocrine therapy, and molecular targeted therapy.³ In the past 2 years, there have also been some emerging treatment methods, such as immunotherapy, antibody-drug conjugates, and so on.^{4,5} Despite advancements in diagnostic techniques and therapeutic strategies for breast cancer, patients continue to experience distant metastases and recurrence, resulting in a poor prognosis.⁶ Therefore, identifying effective treatment methods or therapeutic targets for breast cancer remains an urgent challenge. Ongoing research efforts are focused on identifying effective therapeutic biomarkers to personalize treatment options and establish a comprehensive approach to effectively manage breast cancer.

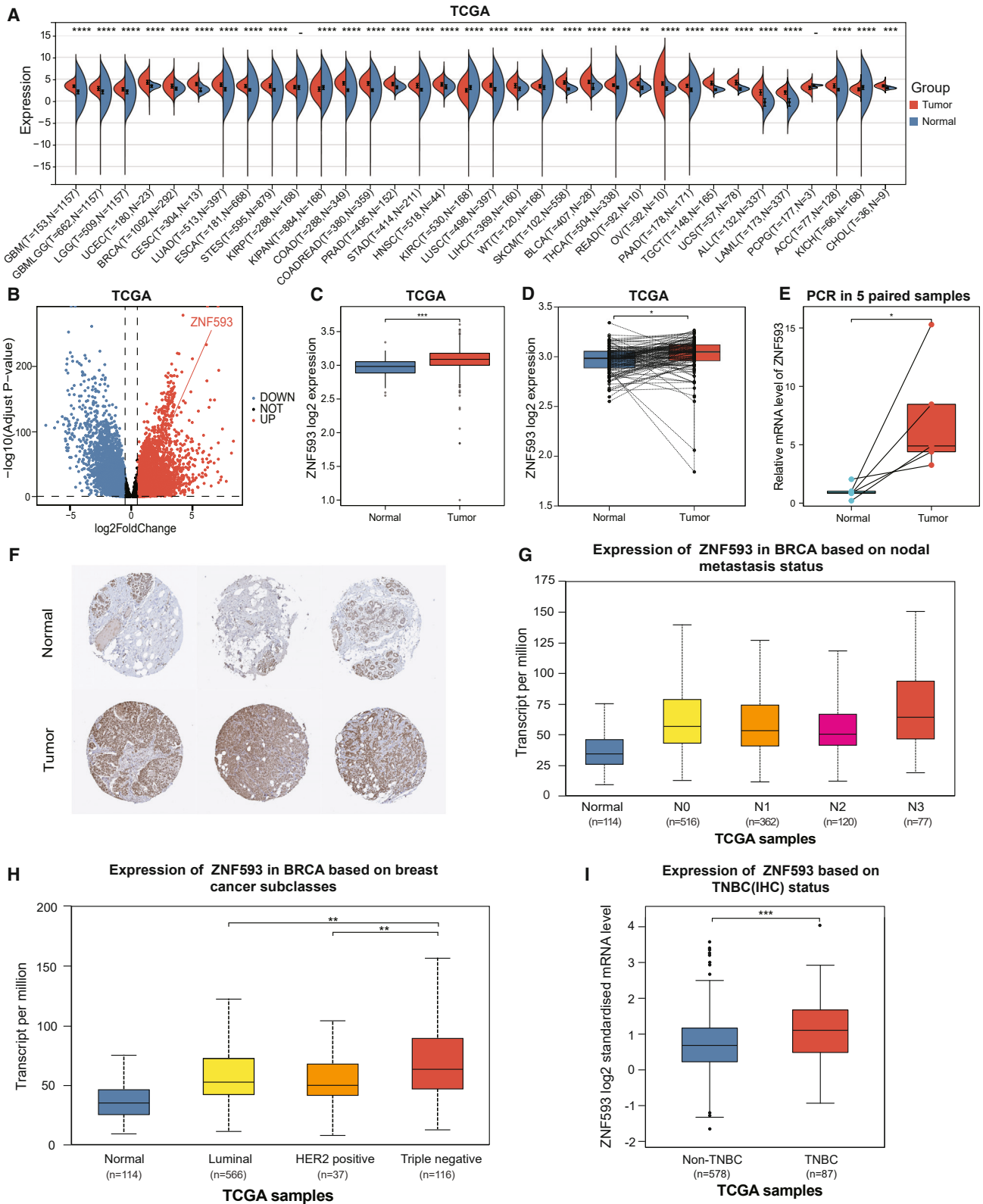
Zinc finger proteins, encoding a group of evolutionarily conserved proteins that present in approximately 5% of all human proteins, exhibit a remarkable binding affinity for a diverse array of substrates, ranging from DNA, RNA, and lipids to

post-translational modifications.⁷ Members of zinc finger proteins play critical roles in various cellular processes, encompassing transcriptional regulation, signal transduction, and cell migration.⁸ Zinc finger proteins have also been shown to play important roles in tumorigenesis and cancer progression.⁹ Current studies have shown that ZNF384, ZNF827, ZCCHC4, and other zinc finger proteins usually promote the proliferation, migration, and chemotherapy tolerance of breast cancer by affecting genome stability and cell-cycle progression.^{10–12}

Here, we identify ZNF593 as an understudied oncogene and regulator of DNA damage process in breast cancer, which is a member of zinc finger proteins family. ZNF593 was discovered by Terunuma et al. in 1997 as a factor that exhibits significant negative regulation of Oct-2 DNA-binding activity.¹³ Subsequent studies indicated that ZNF593 affects the activity of DNA- or RNA-binding proteins through its binding to conserved DNA structures.¹⁴ However, the functional roles of ZNF593 in tumorigenesis remain largely unknown, and no research has yet established a relationship between ZNF593 and DNA damage repair. Our study aims to provide insight into the fundamental role of ZNF593 in breast cancer, with the anticipation of providing new therapeutic targets for breast cancer.

ZNF593 expression was significantly upregulated in cancerous tissues compared to adjacent normal tissues, correlating with





(legend on next page)

poor prognoses in breast cancer. Knockdown of ZNF593 suppressed breast cell proliferation and migration. Mechanistically, ZNF593 enhanced DNA homologous recombination repair, affecting sensitivity to DNA-damage-related chemotherapy. Moreover, our study revealed that ZNF593 regulated the expression of CCND1, CCNE1, and CCNA2, genes encoding cyclins that facilitate the G1/S transition, leading to cell-cycle progression. Additionally, ZNF593 modulated the tumor microenvironment. Collectively, our findings uncovered an oncogenic role of ZNF593 in breast cancer and propose targeting ZNF593 as a promising strategy to overcome chemoresistance in breast cancer.

RESULTS

ZNF593 is overexpressed in breast cancer and is associated with advanced clinicopathological features

First, we analyzed the expression levels of ZNF593 in 34 common tumors and their adjacent normal tissues (Figure 1A). The expression of ZNF593 was significantly increased with a $p < 0.0001$ in 29 types of cancer, including breast invasive carcinoma (BRCA). Next, we found that ZNF593 was significantly up-regulated in breast cancer tissues compared with adjacent normal tissues (Figures 1B and 1C). The correlation was also determined in 96 paired samples (Figure 1D). Later, we utilized quantitative real-time PCR (qPCR) experiments to validate the expression levels of ZNF593 in breast cancer specimens and matched adjacent normal tissues (Figure 1E), which led to the same conclusion. At the protein expression level, the immunohistochemistry (IHC) images of ZNF593 from the Human Protein Atlas (HPA) database also supported the aforementioned conclusions (Figure 1F). In addition, western blot analysis was performed on three pairs of breast cancer and adjacent normal tissues, and it was found that the expression of ZNF593 was increased in cancer tissues (Figure S1E). Our previous conclusion was supported by deeper staining in breast cancer tissue compared to adjacent normal tissues. We then analyzed the relationship between common clinical indicators and the expression of ZNF593. Considering lymph node metastasis status, the results showed that there was no significant difference in the expression of ZNF593 among various lymph node metastasis status. However, there was a trend of high expression in N3 group (Figure 1G). Considering biological subtypes, luminal and HER2-positive subtype breast cancers exhibited a significant decrease in ZNF593 expression compared to triple-negative breast cancer (TNBC) ($p < 0.01$) (Figure 1H). This indicated that ZNF593 was associated with advanced clinicopathological

features. We further analyzed the expression of ZNF593 in TNBC, finding a significant difference compared to adjacent normal tissues ($p = 0.0002$) (Figure 1I). Additionally, the expression of ZNF593 was significantly higher in premenopausal breast cancer patients compared to perimenopausal patients (Figure S1A). But there were no significant differences in ZNF593 expression among different groups in terms of patient age (Figure S1B) and breast cancer stage (Figure S1C). In summary, ZNF593 is highly expressed in breast cancer tissues, and this high expression is associated with breast cancer subtypes, especially within TNBC.

Higher expression of ZNF593 is associated with poorer survival outcome in breast cancer

Kaplan-Meier (KM) plotter survival analysis indicated that high expression of ZNF593 was associated with worse overall survival (OS) and relapse-free survival (RFS) in The Cancer Genome Atlas (TCGA) database (Figures 2A and 2B) and GSE1456 dataset obtained from Gene Expression Omnibus (GEO) database (Figures 2C and 2D). Additionally, we collected surgical samples from 66 breast cancer patients and performed IHC analysis of ZNF593 protein expression (Figure 2E). KM survival analysis further validated that breast cancer patients with high expression of ZNF593 have worse OS and disease-free survival (DFS) (Figures 2F and 2G), which is consistent with our results in the public database. And we also analyzed the relationship between the expression levels of ZNF593 and the survival prognosis in TNBC, obtaining the same results (Figure S1D). In short, these results suggest that breast cancer patients with high levels of ZNF593 tend to have worse survival outcomes.

ZNF593 promotes cell proliferation and migration in breast cancer

With two independent siRNAs, we determined the functions of endogenous ZNF593 by knocking down ZNF593 in MDA-MB-231 and SUM159PT cells (Figures 3A and 3B), which was also verified at the protein level by western blot assay (Figures 3C and 3D). Subsequently, in the cell counting kit-8 (CCK-8) experiment, we compared the results of the control group (siNC) and two experimental groups with ZNF593 knockdown (siZNF593#1, siZNF593#2) and concluded that the cell viability of the two ZNF593 knockdown groups was significantly lower than that of the control group (Figures 3E and 3F). Ablation of ZNF593 dramatically reduced cell proliferation. In addition, migration assays were performed for both cell lines using uncoated transwell chambers. Using representative images (Figure 3G) and

Figure 1. ZNF593 is overexpressed in breast cancer and is associated with advanced clinicopathological features

(A) A pan-cancer analysis of ZNF593 mRNA expression level in 34 cancers.

(B) Differential gene analysis in breast cancer according to the cancer genome atlas (TCGA) database (TCGA:BRCA).

(C and D) Unpair comparison and pair comparison of ZNF593 expression in normal mammary tissues and BC.

(E) The ZNF593's PCR assay of five pairs of cancer and adjacent normal tissues from breast cancer.

(F) IHC staining images of ZNF593 in breast cancer tissue and normal mammary tissue from the HPA database (HPA: <https://www.proteinatlas.org>).

(G) Expression of ZNF593 in BRCA based on nodal metastasis status.

(H) Expression of ZNF593 in BRCA based on breast cancer subclasses.

(I) Expression of ZNF593 based on TNBC (IHC) status. * $p < 0.05$; ** $p < 0.01$; *** $p < 0.001$; **** $p < 0.0001$ by two-tailed Student's t test or two-way ANOVA test. Data are represented as mean \pm SD.

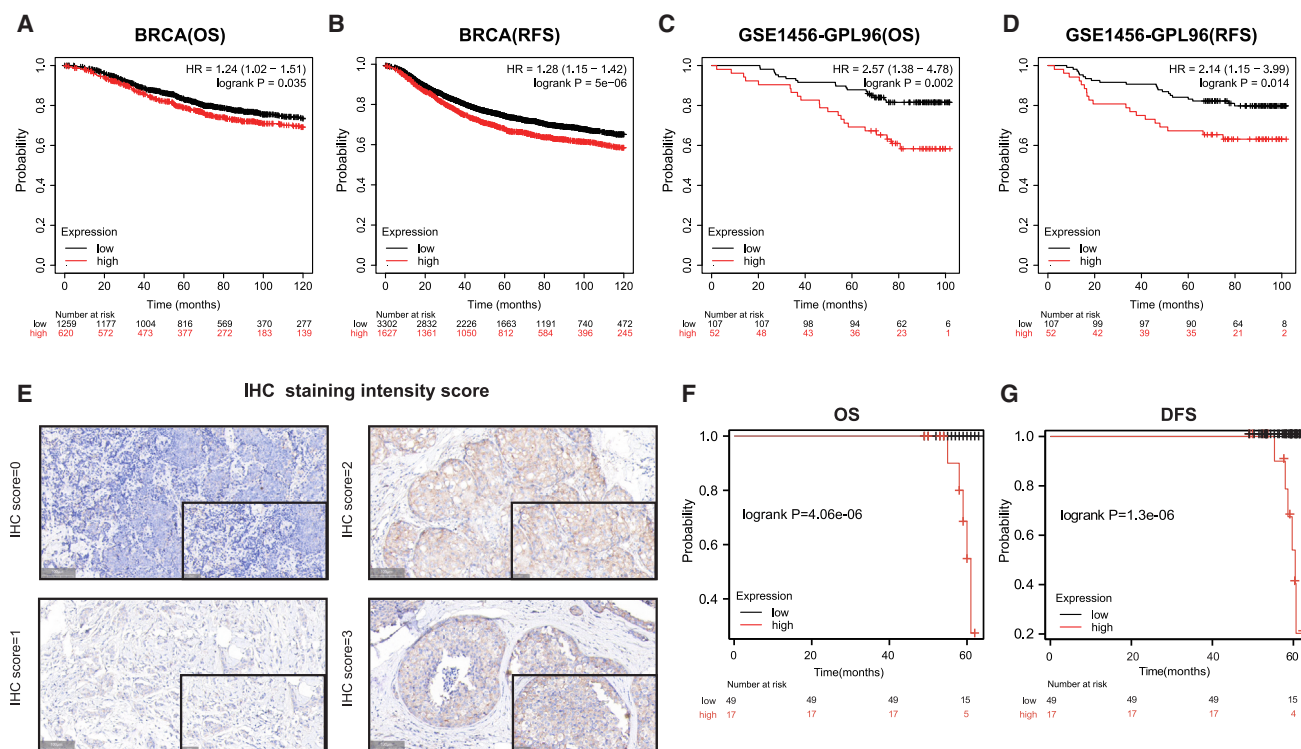


Figure 2. Higher expression of ZNF593 is correlated with poor survival in breast cancer patients

(A and B) Kaplan-Meier plots of ZNF593 in breast cancer according to overall survival (OS) and relapse-free survival (RFS) (KM plotter: <https://kmplot.com/analysis/>). Log rank test.

(C and D) OS and RFS of breast cancer patients analyzed by the GSE1456 dataset (GEO: GSE1456). Log rank test.

(E) IHC staining analysis of ZNF593 expression in 66 breast cancer patients. Representative images are shown. Scale bar: 100 μ m. The scale length of the small image in the bottom right corner of each picture is 50 μ m.

(F and G) Higher expression level of ZNF593 is associated with poor OS and disease-free survival (DFS). Log rank test.

corresponding quantitative results (Figures 3H and 3I), we found that knocking out ZNF593 reduced the migration potential of both cell lines. These results suggest that loss of ZNF593 inhibits the growth and development of breast cancer.

Co-expression network and enrichment analysis of ZNF593

We first used Linkedomics to analyze the top 50 genes positively and negatively correlated with ZNF593 expression in breast cancer tissues (Figures 4A and 4B). With these 100 genes, we performed Gene Ontology (GO) and Kyoto Encyclopedia of Genes and Genomes (KEGG) enrichment analyses (Figure 4C). In terms of GO-molecular function (MF), ZNF593 and its related genes were enriched in DNA-binding transcription factor binding pathway. In GO-biological process (BP), they were enriched in pathways associated with genome stabilization, including ATP biosynthetic process, phosphorylation, subtelomeric heterochromatin formation, DNA damage response, mRNA transcription, and DNA-templated DNA replication. In addition, the cell-cycle-related pathways including mitotic cell-cycle process were also enriched. In GO-cellular component (CC), ZNF593 was enriched at the double-strand break site. GO (Figures S2A and S2C) and KEGG (Figures S2B and S2D) analyses in the GSE1456 and FUSCC-TNBC datasets yielded the same conclusions. Subse-

quently, we conducted protein-protein interaction (PPI) analysis on ZNF593 and found 20 proteins associated with it, of which PRDX4¹⁵ and LTA4H¹⁶ are related to the body's immune system, NSD2¹⁷ is related to the DNA damage repair process, cGAS is both related to DNA damage repair¹⁸ and immune system,¹⁹ SSB²⁰ and DNPH1²¹ are involved in the nucleic acid binding and metabolism process, and USO1 plays a role in the mitosis process²² (Figure 4D). In summary, ZNF593 plays a role not only in maintaining genomic stability but also in the regulation of cell cycle and has a certain impact on the function of the immune system.

ZNF593 promotes DNA damage repair

Gene set enrichment analysis (GSEA) indicated that ZNF593 was significantly enriched in pathways related to DNA repair (Figures 5A and S3A), DNA damage response (Figures 5B and 5D), and DNA recombination (Figure 5C). Furthermore, we performed enrichment analysis using GSE1456 dataset (Figures S3B and C) and FUSCC-TNBC dataset (Figure S3D), which also showed enrichment of ZNF593 in pathways related to DNA damage repair. Subsequently, single-sample GSEA (ssGSEA) analysis of the TCGA and FUSCC-TNBC database revealed that ZNF593 was associated with a homologous recombination (HR) repair pathway in DNA damage repair (Figures 5E and 5F). Subsequently, we used western blot

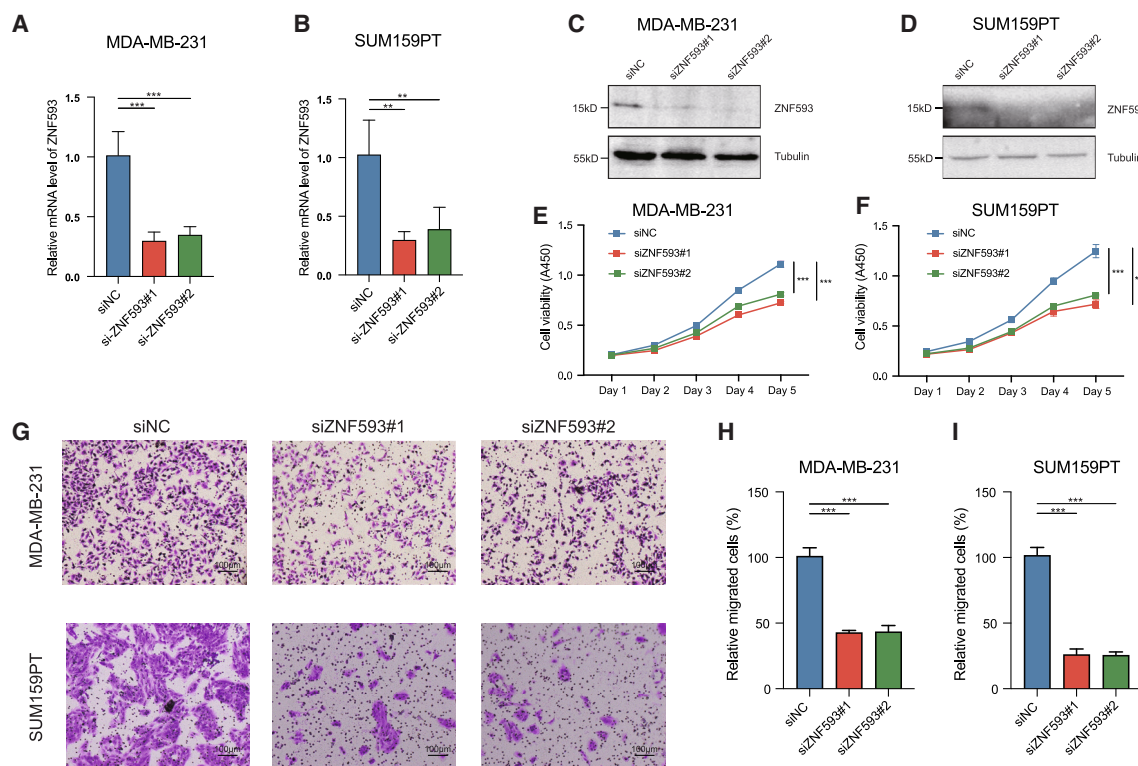


Figure 3. ZNF593 deficiency inhibits cell proliferation and migration in breast cancer

(A and B) ZNF593 expression was confirmed via RT-qPCR analysis in MDA-MB-231 and SUM159PT cells transfected with two distinct siRNAs targeting ZNF593. (C and D) Western blot verified that both of the above two distinct siRNAs could knock down ZNF593 at the protein level. (E and F) Knockdown of ZNF593 suppresses cell proliferation in MDA-MB-231 and SUM159PT cells, as assessed by cell counting kit-8 assays. (G) Knockdown of ZNF593 suppresses migration ability of MDA-MB-231 and SUM159PT cells by migration assays. Scale bar: 100 μ m. (H and I) Corresponding quantitative results of migration ability in MDA-MB-231 and SUM159PT cells are shown. ** $p < 0.01$; *** $p < 0.001$ by two-tailed Student's *t* test or two-way ANOVA test. Data are represented as mean \pm SD.

experiments to observe that intracellular γ H2AX protein expression increased after ZNF593 knockdown (Figures 5G and 5H). In exploring the mechanism of this process, we found that RAD50 decreased with the decrease of ZNF593 (Figures 5I and 5J). Based on these findings, we performed drug sensitivity analysis on MDA-MB-231 and SUM159PT cells using cisplatin and carboplatin, which target the DNA damage repair process.²³ ZNF593 knockdown enhances the sensitivity of breast cancer cells to cisplatin (Figures 5K and 5M) and carboplatin (Figures 5L and 5N). Collectively, ZNF593 promotes DNA damage repair, thus affecting drug sensitivity.

ZNF593 regulates cell-cycle progression

Moreover, GSEA indicated that ZNF593 was enriched in cell-cycle-related pathways, including processes such as mitosis/meiosis and cell-cycle checkpoint regulation (Figures 6A–6G). Next, we verified the aforementioned conclusions by flow cytometry analysis of cell cycle in MDA-MB-231 and SUM159PT cells. Depletion of ZNF593 triggered an accumulation of cell cycle at G1 phase in MDA-MB-231 and SUM159PT cells (Figure 6H). Mechanistically, depletion of ZNF593 repressed the expression of CCND1, CCNE1, and CCNA2, genes encoding cyclins that promote the G1/S transition²⁴ (Figures 6K and 6L). In

summary, ZNF593 regulates cell-cycle progression by controlling the expression of cell-cycle-associated genes.

ZNF593 is associated with immune environment

ZNF593 was found to interact with immune-related proteins by PPI analysis. Immune score analysis showed that ESTIMATE score was lower in samples with higher expression of ZNF593, which indicated negative effect of ZNF593 on the formation of tumor immune environment (Figure 7A). Subsequently, we performed ssGSEA using TCGA and FUSCC-TNBC databases, showing that low expression of ZNF593 was enriched in pathways associated with immune memory and tumor immune response (Figures 7B and 7C). We analyzed the correlation between ZNF593 expression and various immune cell markers in breast cancer. ZNF593 expression was negatively correlated with multiple immune cell markers, including MS4A1, CD4, FOXP3, CD86, MRC1, CD68, CD209, and NCAM1.²⁵ Further reverse transcription-PCR (RT-PCR) experiments also proved that ZNF593 might inhibit the formation or function of immune cells (Figures 7E–7P and S4A–S4D). This conclusion suggested that the high expression of ZNF593 inhibits the aggregation or functional formation of immune cells in tumor cells, thus forming a poor tumor immune environment.

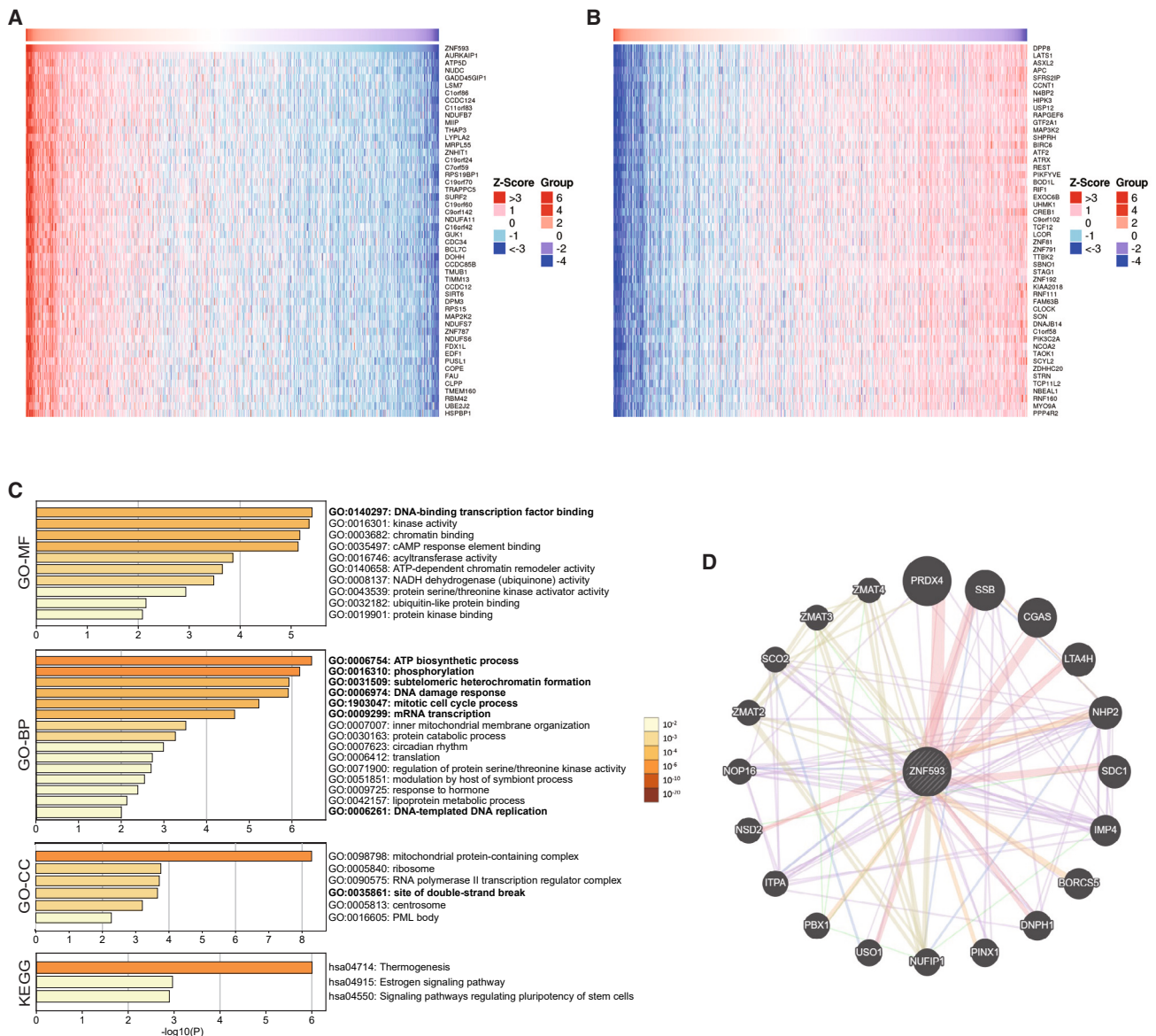


Figure 4. Co-expression analysis, enrichment analysis, and protein-protein interaction analysis of ZNF593

(A and B) The top 50 genes positively and negatively correlated with ZNF593 expression by Linkedomics (Linkedomics: <http://www.linkedomics.org/login.php>). (C) GO and KEGG enrichment analyses of ZNF593 and its related 100 genes. (D) PPI analysis on ZNF593 in breast cancer.

DISCUSSION

The zinc finger proteins family is a group of sequence-specific DNA-binding proteins that play significant roles in carcinogenesis and cancer progression.²⁶ They are implicated in various aspects, such as DNA damage repair, regulation of cell cycle, and regulation of transcription factors.²⁷ Some zinc finger proteins function as tumor suppressors by regulating genes involved in cell-cycle control²⁸ and apoptosis,²⁹ whereas others promote breast cancer growth and metastasis by fostering an immunosuppressive tumor microenvironment (TME).³⁰ ZNF593, a member of the zinc finger proteins family, has been relatively under-

studied regarding its role in cancer initiation and progression. Although there is a broad understanding of the functions of zinc finger proteins in various cellular processes, research on the role of ZNF593, a member of the zinc finger protein family, in the onset and development of cancer remains largely incomplete. Therefore, more comprehensive studies are needed to elucidate how ZNF593 might affect the initiation and progression of cancer, which could potentially reveal new targets for therapeutic intervention.

Here, we uncovered the role for the ZNF593 in the regulation of breast cancer development and therapy. ZNF593 is upregulated in breast cancer tissues compared with the adjacent normal

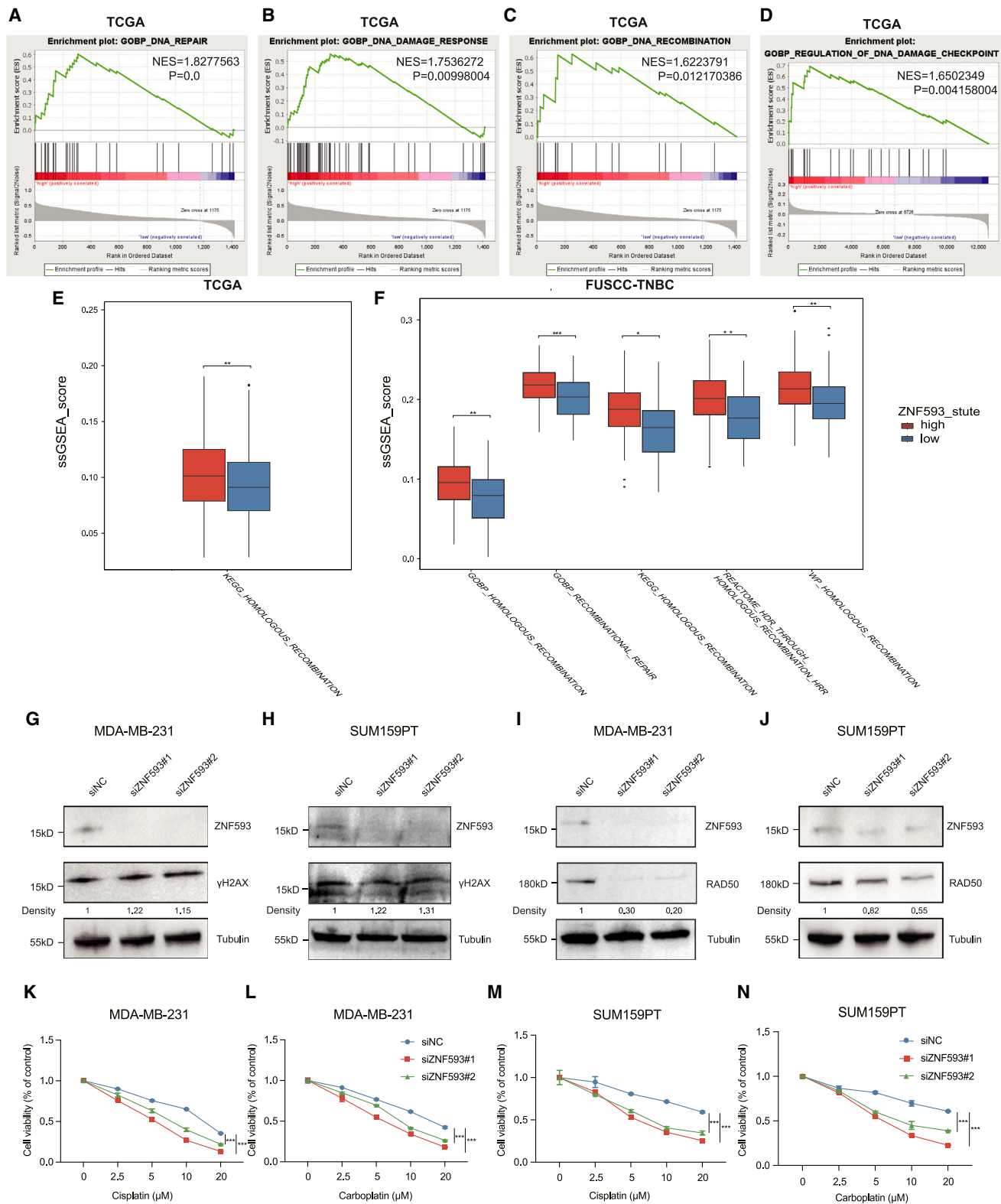


Figure 5. ZNF593 is strongly connected with the DNA damage repair

(A–D) Enrichment plot of ZNF593 about DNA damage repair by GSEA according to TCGA database.

(E and F) ssGSEA of ZNF593 in TCGA and FUSCC-TNBC database about DNA damage repair.

(legend continued on next page)

tissues. Further analysis revealed correlations between ZNF593 expression and clinicopathological features. Particularly, ZNF593 showed a significantly high expression level in TNBC (Figures 1 and S1). Survival analysis determined that high expression levels of ZNF593 in tumors are significantly associated with unfavorable prognoses (Figure 2). Subsequently, CCK-8 and transwell assays were performed to validate that the downregulation of ZNF593 suppresses cell viability and migration ability of breast cancer (Figure 3).

The zinc finger proteins family can recruit and regulate other proteins involved in the DNA damage repair process, ensuring accurate and efficient repair of DNA breaks.³¹ In this study, we demonstrated that ZNF593 indeed plays a promoting role in DNA damage repair. Firstly, the enrichment analysis of TCGA and FUSCC-TNBC databases suggested that ZNF593 was indeed enriched in the pathway associated with DNA damage repair, especially homologous recombination repair (Figures 5A–5F and S3A–S3D). γ H2AX is a marker of DNA damage repair.³² In the western blot experiment (Figures 5G and 5I), we found that when ZNF593 was knocked down, the intracellular expression of γ H2AX was increased, indicating that the loss of ZNF593 may lead to increased DNA damage. The MRN complex is composed of meiosis recombination 11 (MRE11), RAD50, and Nijmegen breakage syndrome 1 (NBS1), also known as nibrin, which is central to maintaining DNA damage repair.³³ In our study, RAD50 was found to decrease with the knockdown of ZNF593. We hypothesized that ZNF593 could affect the formation of MRN recombination by affecting the expression of RAD50 and ultimately affect the progress of DNA damage repair. The abnormality of DNA damage repair function is one of the main mechanisms of chemotherapy resistance.³⁴ Thus, we carried out drug sensitivity assays and found that breast cancer cells with low expression level of ZNF593 showed increased sensitivity to cisplatin and carboplatin (Figures 5K–5N).²³ This further demonstrated that ZNF593 can promote the development of cancer by affecting the DNA damage repair process, and ZNF593 provides a new target for addressing chemotherapy resistance.

Cell-cycle dysregulation is one of the main characteristics of cancer.³⁵ Studies have shown that zinc finger protein can promote cell proliferation by promoting cell-cycle progression in G1 phase and changing the expression of cell-cycle regulators.³⁶ In this paper, we demonstrated that ZNF593 can regulate cell-cycle progression. First, enrichment analysis indicated that ZNF593 was enriched in cell-cycle progression and cell-cycle-checkpoint-related pathways (Figures 6A–6G). To test this hypothesis, we conducted a series of flow cytometry analysis of cell cycle. Intriguingly, depletion of ZNF593 triggered an accumulation of cell cycle at G1 phase in breast cancer cells (Figures 6H–6J). Mechanistically, depletion of ZNF593 repressed the expression of CCND1, CCNE1, and CCNA2, genes encoding cyclins that guarantee G1/S transition (Figures 6K and 6L).³⁷ Our results suggest that overexpression of ZNF593 in breast cancer

promotes cell-cycle progression and highlights the important functions of ZNF593 in tumorigenesis and cancer progression.

In terms of regulation of transcription factors, the existing literature indicates that ZNF593 is a factor that significantly negatively regulates the DNA-binding activity of transcription factor Oct-2.¹³ Oct-2 is a transcriptional activator required for B cell immunoglobulin gene expression.³⁸ Therefore, whether ZNF593 can have an effect on the immune system of tumors is the focus of our investigation. After ESTIMATE immune score, ssGSEA immune pathway enrichment, and correlation of immune cell molecular markers, we found that ZNF593 does affect the formation of tumor-related immune environment. Furthermore, the knockdown of ZNF593 expression is associated with an enhanced tumor immune environment, suggesting that immune cells may exhibit an upward trend in numbers or functionality (Figure 7).

In summary, our study represents report linking ZNF593 with breast cancer progression. Additionally, our research reveals that high expression of ZNF593 in breast cancer samples correlates with poorer patient survival. We found that ZNF593 promotes proliferation and metastasis of breast cancer cells by facilitating cell-cycle progression and DNA damage repair while influencing the tumor immune environment, which needs further investigation into the underlying mechanisms. Compared with other subtypes, ZNF593 may exhibit a more prominent marker and targeting effect in TNBC. Moreover, ZNF593 serves not only as a tumor promoter but also as a potential target to overcome chemoresistance in breast cancer. These findings highlight its significance as a vital biomarker and therapeutic target for diagnosing and treating breast cancer in the future. Overall, ZNF593 emerges as a promising prognostic biomarker and therapeutic target in breast cancer research.

Limitations of the study

First of all, this study only observed the difference between intracellular gene expression after ZNF593 knockdown and non-knockdown, and no experiments related to overexpression of ZNF593 were conducted to verify the conclusion. Second, in addition to the database data, there were only 66 clinical follow-up data in this study, and larger clinical specimens and external datasets were needed to verify the prognostic value of ZNF593 in breast cancer. Finally, this study only preliminarily discussed the effects of ZNF593 on biological behaviors such as breast cancer cell migration and proliferation, as well as the effects on genome stability, cell cycle, and tumor immune environment. Nevertheless, more studies of the underlying mechanisms need to be further refined.

RESOURCE AVAILABILITY

Lead contact

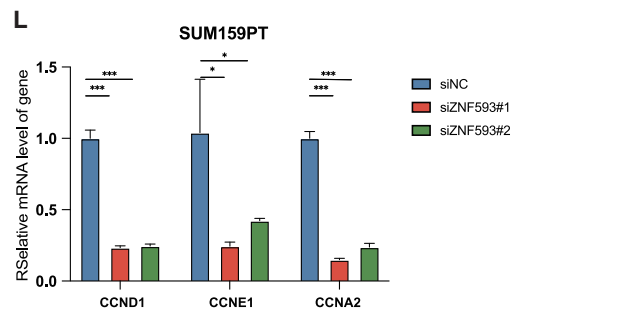
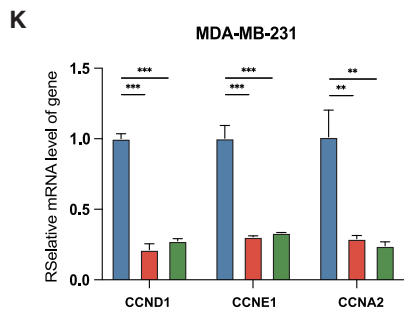
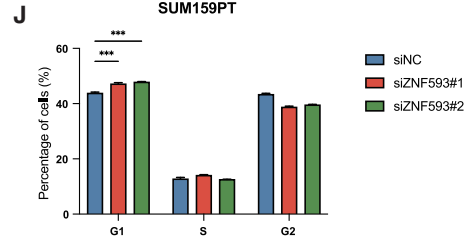
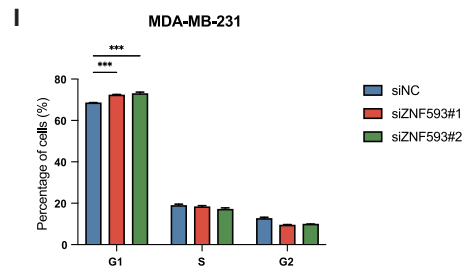
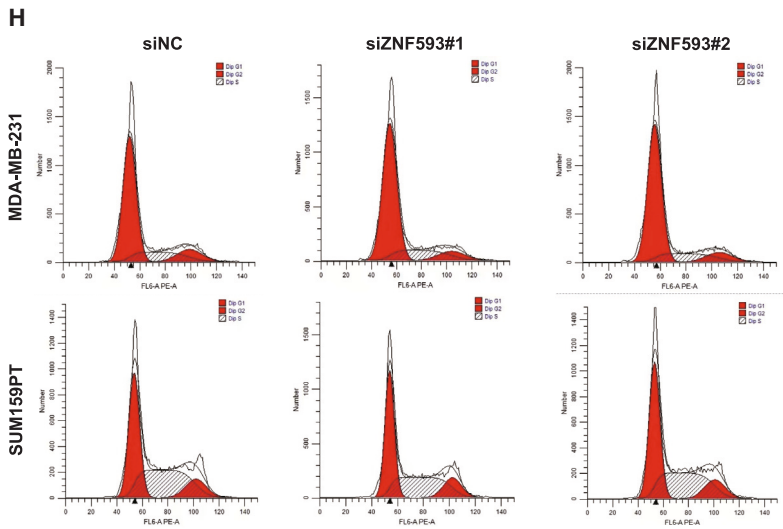
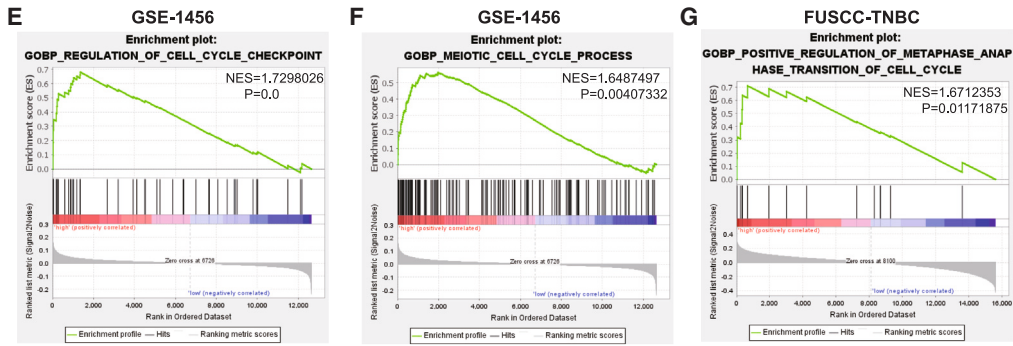
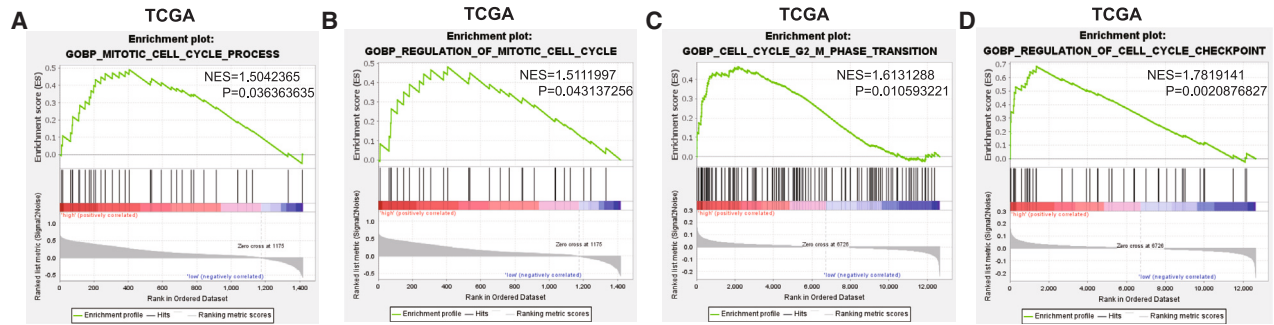
Further information and requests for resources and reagents should be directed to and will be fulfilled by the lead contact, Yingying Xu (xuyingying@cmu.edu.cn).

(G and H) Western blot experiments in MDA-MB-231 and SUM159PT cells confirmed that ZNF593 is involved in DNA damage repair.

(I and J) ZNF593 affects DNA damage repair by affecting RAD50 expression.

(K and L) Drug sensitivity assays of MDA-MB-231 cells before and after ZNF593 knockdown with cisplatin and carboplatin.

(M and N) Drug sensitivity assays of SUM159PT cells before and after ZNF593 knockdown with cisplatin and carboplatin. * $p < 0.05$; ** $p < 0.01$; *** $p < 0.001$ by two-tailed Student's t test or two-way ANOVA test. Data are represented as mean \pm SD.



(legend on next page)

Materials availability

This study did not generate new unique reagents. The materials involved in the article are listed in detail in the [key resources table](#) and the [method details](#) section. Any additional information about this article can be obtained from the [lead contact](#) upon request.

Data and code availability

- This paper analyzes existing, publicly available data.
- This study does not report original code. All codes were used in this study in alignment with recommendations made by authors of R packages in their respective user's guide, which can be accessed at <https://bioconductor.org>.
- Websites or software such as HPA, KM-Plotter, Linkedomics, GeneMANIA, TIMER, ImageJ, and GSEA were employed in this article. Detailed information is mentioned in the [method details](#) section and the [key resources table](#).
- Any additional information required to reanalyze the data used in this study is available from the [lead contact](#) upon request.

ACKNOWLEDGMENTS

This work was supported by the National Natural Science Foundation of China (82203786, 82373231, 82403132), the Natural Science Foundation of Liaoning Province of China (2022-YGJC-68, 2023-BS-105, 2024-BS-060), and Chinese Young Breast Experts Research Project (CYBER-2021-A02, CYBER-2022-001). We thank the laboratory members for active and helpful discussion. And we would like to thank Professor Zhimin Shao of Fudan University Shanghai Cancer Center for his help and guidance to us.

AUTHOR CONTRIBUTIONS

X.L., L.Y., and Y.X. designed research. Y.Z. wrote the paper and carried out data analyses. X.T. designed the experiment and conducted the experiment. C.W. collated the data, designed, and developed the database. M.W. proof-read and reviewed the article. M.L. conducted partial experiments. All authors have read and approved the final submitted manuscript.

DECLARATION OF INTERESTS

The authors declare no competing interests.

STAR★METHODS

Detailed methods are provided in the online version of this paper and include the following:

- [KEY RESOURCES TABLE](#)
- [EXPERIMENTAL MODEL AND STUDY PARTICIPANT DETAILS](#)
- [METHOD DETAILS](#)
 - Datasets
 - Breast cancer samples
 - Differential analysis of ZNF593 expression
 - Survival analysis
 - Functional analysis
 - RNA isolation and quantitative reverse transcription polymerase chain reaction (RT-qPCR)
 - Western blotting

- ImageJ
- Cell viability
- Transwell migration assays
- Flow cytometry analysis

● QUANTIFICATION AND STATISTICAL ANALYSIS

SUPPLEMENTAL INFORMATION

Supplemental information can be found online at <https://doi.org/10.1016/j.isci.2024.111513>.

Received: July 1, 2024

Revised: September 12, 2024

Accepted: November 28, 2024

Published: December 3, 2024

REFERENCES

1. Siegel, R.L., Giaquinto, A.N., and Jemal, A. (2024). Cancer statistics, 2024. *CA A Cancer J. Clin.* 74, 12–49. <https://doi.org/10.3322/caac.21820>.
2. Wu, J., Fan, D., Shao, Z., Xu, B., Ren, G., Jiang, Z., Wang, Y., Jin, F., Zhang, J., Zhang, Q., et al. (2022). CACA Guidelines for Holistic Integrative Management of Breast Cancer. *Holist. Integr. Oncol.* 1, 7. <https://doi.org/10.1007/s44178-022-00007-8>.
3. Veronesi, U., Boyle, P., Goldhirsch, A., Orecchia, R., and Viale, G. (2005). Breast cancer. *Lancet (London, England)* 365, 1727–1741.
4. Semiglazov, V., Tseluiko, A., Kudaybergenova, A., Artemyeva, A., Krivorotko, P., and Donskih, R. (2022). Immunology and immunotherapy in breast cancer. *Cancer Biol. Med.* 19, 609–618. <https://doi.org/10.20892/j.issn.2095-3941.2021.0597>.
5. Chang, H.L., Schwettmann, B., McArthur, H.L., and Chan, I.S. (2023). Antibody-drug conjugates in breast cancer: overcoming resistance and boosting immune response. *J. Clin. Invest.* 133, e172156. <https://doi.org/10.1172/jci172156>.
6. Johnston, S.R.D., Harbeck, N., Hegg, R., Toi, M., Martin, M., Shao, Z.M., Zhang, Q.Y., Martinez Rodriguez, J.L., Campone, M., Hamilton, E., et al. (2020). Abemaciclib Combined With Endocrine Therapy for the Adjuvant Treatment of HR+, HER2-Node-Positive, High-Risk, Early Breast Cancer (monarchE). *J. Clin. Oncol.* 38, 3987–3998. <https://doi.org/10.1200/jco.20.02514>.
7. Vilas, C.K., Emery, L.E., Denchi, E.L., and Miller, K.M. (2018). Caught with One's Zinc Fingers in the Genome Integrity Cookie Jar. *Trends Genet.* 34, 313–325. <https://doi.org/10.1016/j.tig.2017.12.011>.
8. Cassandri, M., Smirnov, A., Novelli, F., Pitolli, C., Agostini, M., Malewicz, M., Melino, G., and Raschella, G. (2017). Zinc-finger proteins in health and disease. *Cell Death Dis.* 3, 17071. <https://doi.org/10.1038/cddiscovery.2017.71>.
9. Zhao, J., Wen, D., Zhang, S., Jiang, H., and Di, X. (2023). The role of zinc finger proteins in malignant tumors. *Faseb. J.* 37, e23157. <https://doi.org/10.1096/fj.202300801R>.
10. Singh, J.K., Smith, R., Rother, M.B., de Groot, A.J.L., Wiegant, W.W., Vreeken, K., D'Augustin, O., Kim, R.Q., Qian, H., Krawczyk, P.M., et al. (2021). Zinc finger protein ZNF384 is an adaptor of Ku to DNA during

Figure 6. ZNF593 regulates cell-cycle progression in breast cancer cell

(A–D) Enrichment plot of ZNF593 about cell-cycle progression by GSEA according to TCGA database.

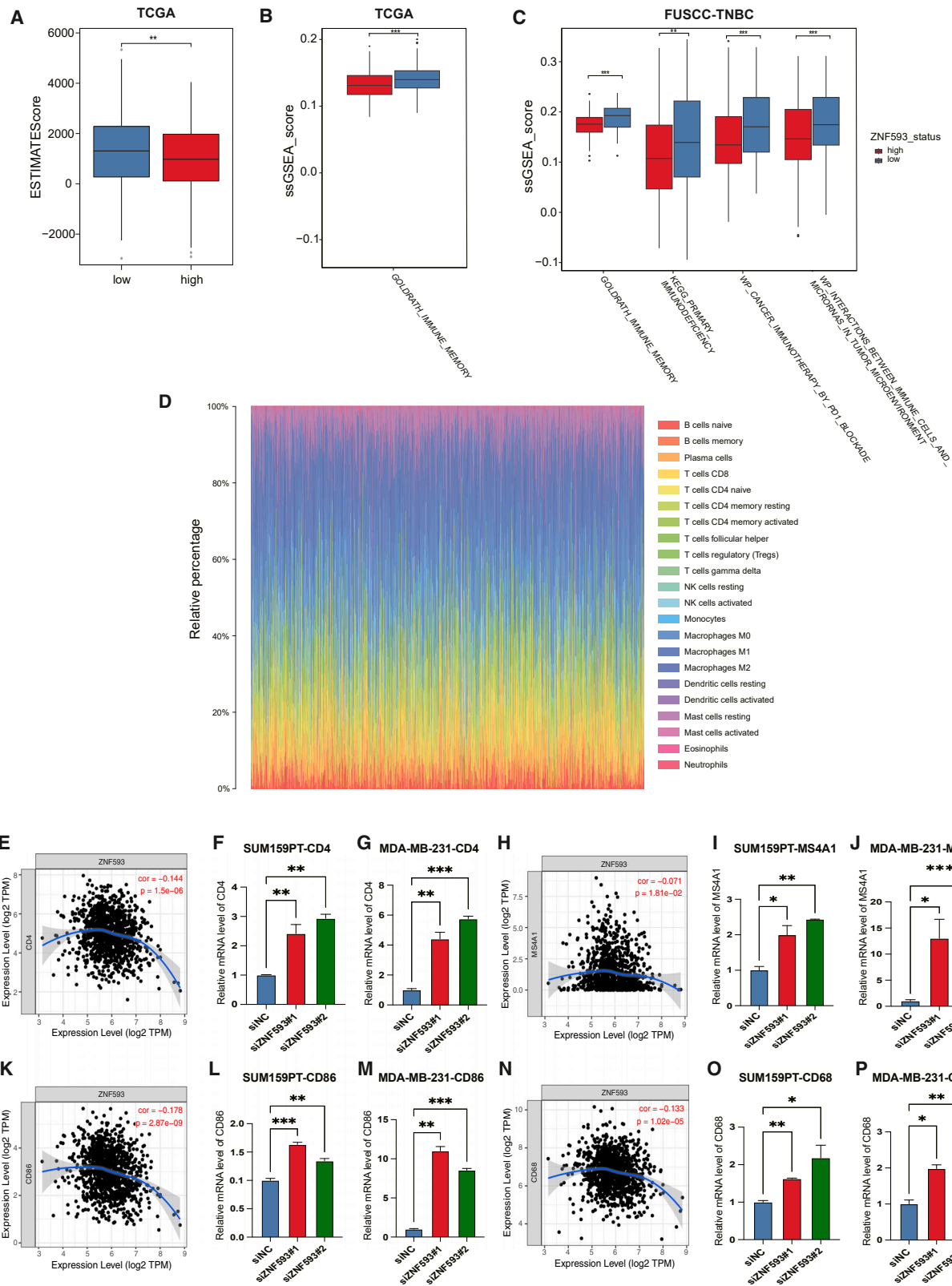
(E–G) GSEA of ZNF593 in GSE1456 and FUSCC-TNBC database about cell-cycle progression.

(H) Knockdown of ZNF593 results in cell-cycle arrest at the G1 phase in MDA-MB-231 and SUM159PT cells, as demonstrated by flow cytometry analysis using propidium iodide (PI) staining. The percentage of cells in the G1/S/G2 phase are shown.

(I and J) Corresponding quantitative results of flow cytometry analysis in MDA-MB-231 and SUM159PT cells are shown.

(K and L) Knockdown of ZNF593 represses the mRNA expression of CCND1, CCNE1, and CCNA2 in MDA-MB-231 and SUM159PT cells by RT-qPCR analysis.

* $p < 0.05$; ** $p < 0.01$; *** $p < 0.001$ by two-tailed Student's t test or two-way ANOVA test. Data are represented as mean \pm SD.



(legend on next page)

- classical non-homologous end-joining. *Nat. Commun.* 12, 6560. <https://doi.org/10.1038/s41467-021-26691-0>.
11. Yang, S.F., Nelson, C.B., Wells, J.K., Fernando, M., Lu, R., Allen, J.A.M., Malloy, L., Lamm, N., Murphy, V.J., Mackay, J.P., et al. (2024). ZNF827 is a single-stranded DNA binding protein that regulates the ATR-CHK1 DNA damage response pathway. *Nat. Commun.* 15, 2210. <https://doi.org/10.1038/s41467-024-46578-0>.
 12. Zhu, H., Chen, K., Chen, Y., Liu, J., Zhang, X., Zhou, Y., Liu, Q., Wang, B., Chen, T., and Cao, X. (2022). RNA-binding protein ZCCHC4 promotes human cancer chemoresistance by disrupting DNA-damage-induced apoptosis. *Signal Transduct. Targeted Ther.* 7, 240. <https://doi.org/10.1038/s41392-022-01033-8>.
 13. Terunuma, A., Shiba, K., and Noda, T. (1997). A novel genetic system to isolate a dominant negative effector on DNA-binding activity of Oct-2. *Nucleic Acids Res.* 25, 1984–1990.
 14. Hayes, P.L., Lytle, B.L., Volkman, B.F., and Peterson, F.C. (2008). The solution structure of ZNF593 from *Homo sapiens* reveals a zinc finger in a predominantly unstructured protein. *Protein Sci.* 17, 571–576. <https://doi.org/10.1110/ps.073290408>.
 15. Lipinski, S., Pfeuffer, S., Arnold, P., Treitz, C., Aden, K., Ebsen, H., Falk-Paulsen, M., Gisch, N., Fazio, A., Kuiper, J., et al. (2019). Prdx4 limits caspase-1 activation and restricts inflammasome-mediated signaling by extracellular vesicles. *EMBO J.* 38, e101266. <https://doi.org/10.15252/embj.2018101266>.
 16. Guo, Z., Huang, J., Huo, X., Huang, C., Yu, X., Sun, Y., Li, Y., He, T., Guo, H., Yang, J., and Xue, L. (2024). Targeting LTA4H facilitates the reshaping of the immune microenvironment mediated by CCL5 and sensitizes ovarian cancer to Cisplatin. *Sci. China Life Sci.* 67, 1226–1241. <https://doi.org/10.1007/s11427-023-2444-5>.
 17. Zhang, J., Lee, Y.R., Dang, F., Gan, W., Menon, A.V., Katon, J.M., Hsu, C.H., Asara, J.M., Tibarewal, P., Leslie, N.R., et al. (2019). PTEN Methylation by NSD2 Controls Cellular Sensitivity to DNA Damage. *Cancer Discov.* 9, 1306–1323. <https://doi.org/10.1158/2159-8290.Cd-18-0083>.
 18. Li, T., and Chen, Z.J. (2018). The cGAS-cGAMP-STING pathway connects DNA damage to inflammation, senescence, and cancer. *J. Exp. Med.* 215, 1287–1299. <https://doi.org/10.1084/jem.20180139>.
 19. Du, M., and Chen, Z.J. (2018). DNA-induced liquid phase condensation of cGAS activates innate immune signaling. *Science* 361, 704–709. <https://doi.org/10.1126/science.aat1022>.
 20. Thrall, E.S., Piatt, S.C., Chang, S., and Loparo, J.J. (2022). Replication stalling activates SSB for recruitment of DNA damage tolerance factors. *Proc. Natl. Acad. Sci. USA* 119, e2208875119. <https://doi.org/10.1073/pnas.2208875119>.
 21. Fugger, K., Bajrami, I., Silva Dos Santos, M., Young, S.J., Kunzelmann, S., Kelly, G., Hewitt, G., Patel, H., Goldstone, R., Carell, T., et al. (2021). Targeting the nucleotide salvage factor DNPH1 sensitizes BRCA-deficient cells to PARP inhibitors. *Science* 372, 156–165. <https://doi.org/10.1126/science.abb4542>.
 22. Jin, Y., and Dai, Z. (2016). USO1 promotes tumor progression via activating Erk pathway in multiple myeloma cells. *Biomed. Pharmacother.* 78, 264–271. <https://doi.org/10.1016/j.biopha.2016.01.012>.
 23. Rotenberg, S., Disler, C., and Perego, P. (2021). The rediscovery of platinum-based cancer therapy. *Nat. Rev. Cancer* 21, 37–50. <https://doi.org/10.1038/s41568-020-00308-y>.
 24. Martínez-Alonso, D., and Malumbres, M. (2020). Mammalian cell cycle cyclins. *Semin. Cell Dev. Biol.* 107, 28–35. <https://doi.org/10.1016/j.semcdb.2020.03.009>.
 25. Zilionis, R., Engblom, C., Pfirschke, C., Savova, V., Zemmour, D., Saaticoglu, H.D., Krishnan, I., Maroni, G., Meyerovitz, C.V., Kerwin, C.M., et al. (2019). Single-Cell Transcriptomics of Human and Mouse Lung Cancers Reveals Conserved Myeloid Populations across Individuals and Species. *Immunity* 50, 1317–1334.e10. <https://doi.org/10.1016/j.immuni.2019.03.009>.
 26. Wu, H.T., Zhong, H.T., Li, G.W., Shen, J.X., Ye, Q.Q., Zhang, M.L., and Liu, J. (2020). Oncogenic functions of the EMT-related transcription factor ZEB1 in breast cancer. *J. Transl. Med.* 18, 51. <https://doi.org/10.1186/s12967-020-02240-z>.
 27. Jen, J., and Wang, Y.C. (2016). Zinc finger proteins in cancer progression. *J. Biomed. Sci.* 23, 53. <https://doi.org/10.1186/s12929-016-0269-9>.
 28. Liu, H.Y., Liu, Y.Y., Yang, F., Zhang, L., Zhang, F.L., Hu, X., Shao, Z.M., and Li, D.Q. (2020). Acetylation of MORC2 by NAT10 regulates cell-cycle checkpoint control and resistance to DNA-damaging chemotherapy and radiotherapy in breast cancer. *Nucleic Acids Res.* 48, 3638–3656. <https://doi.org/10.1093/nar/gkaa130>.
 29. Fan, J., Zhang, Z., Chen, H., Chen, D., Yuan, W., Li, J., Zeng, Y., Zhou, S., Zhang, S., Zhang, G., et al. (2024). Zinc finger protein 831 promotes apoptosis and enhances chemosensitivity in breast cancer by acting as a novel transcriptional repressor targeting the STAT3/Bcl2 signaling pathway. *Genes Dis.* 17, 430–448. <https://doi.org/10.1016/j.gendis.2022.11.023>.
 30. Jiang, H., Wei, H., Wang, H., Wang, Z., Li, J., Ou, Y., Xiao, X., Wang, W., Chang, A., Sun, W., et al. (2022). Zeb1-induced metabolic reprogramming of glycolysis is essential for macrophage polarization in breast cancer. *Cell Death Dis.* 13, 206. <https://doi.org/10.1038/s41419-022-04632-z>.
 31. Moison, C., Chagraoui, J., Caron, M.C., Gagné, J.P., Coulombe, Y., Poirier, G.G., Masson, J.Y., and Sauvageau, G. (2021). Zinc finger protein E4F1 cooperates with PARP-1 and BRG1 to promote DNA double-strand break repair. *Proc. Natl. Acad. Sci. USA* 118, e2019408118. <https://doi.org/10.1073/pnas.2019408118>.
 32. Natale, F., Rapp, A., Yu, W., Maiser, A., Harz, H., Scholl, A., Grulich, S., Anton, T., Hörl, D., Chen, W., et al. (2017). Identification of the elementary structural units of the DNA damage response. *Nat. Commun.* 8, 15760. <https://doi.org/10.1038/ncomms15760>.
 33. Stracker, T.H., and Petrini, J.H.J. (2011). The MRE11 complex: starting from the ends. *Nat. Rev. Mol. Cell Biol.* 12, 90–103. <https://doi.org/10.1038/nrm3047>.
 34. Goldstein, M., and Kastan, M.B. (2015). The DNA damage response: implications for tumor responses to radiation and chemotherapy. *Annu. Rev. Med.* 66, 129–143. <https://doi.org/10.1146/annurev-med-081313-121208>.
 35. Matthews, H.K., Bertoli, C., and de Bruin, R.A.M. (2022). Cell cycle control in cancer. *Nat. Rev. Mol. Cell Biol.* 23, 74–88. <https://doi.org/10.1038/s41580-021-00404-3>.
 36. Luo, A., Zhang, X., Fu, L., Zhu, Z., and Dong, J.T. (2016). Zinc finger factor ZNF121 is a MYC-interacting protein functionally affecting MYC and cell proliferation in epithelial cells. *J. Genet. Genomics.* 43, 677–685. <https://doi.org/10.1016/j.jgg.2016.05.006>.

Figure 7. ZNF593 inhibits the formation of tumor immune environment

(A) ESTIMATE score analysis in breast cancer according to ZNF593 expression level.

(B and C) ssGSEA of ZNF593 in TCGA and FUSCC-TNBC database about immune environment.

(D) Percentage of 22 types of immune cells in breast cancer patients.

(E, H, K, and N) Correlation between many immune cell markers and ZNF593 in breast cancer tissues.

(F and G, I and J, L and M, and O and P) RT-qPCR was used to verify the relationship between the immune markers and ZNF593. * $p < 0.05$; ** $p < 0.01$; *** $p < 0.001$ by two-tailed Student's t test or two-way ANOVA test. Data are represented as mean \pm SD.

37. Bertoli, C., Skotheim, J.M., and de Bruin, R.A.M. (2013). Control of cell cycle transcription during G1 and S phases. *Nat. Rev. Mol. Cell Biol.* *14*, 518–528. <https://doi.org/10.1038/nrm3629>.
38. Corcoran, L.M., and Karvelas, M. (1994). Oct-2 is required early in T cell-independent B cell activation for G1 progression and for proliferation. *Immunity* *7*, 635–645. [https://doi.org/10.1016/1074-7613\(94\)90035-3](https://doi.org/10.1016/1074-7613(94)90035-3).
39. Vasaikar, S.V., Straub, P., Wang, J., and Zhang, B. (2018). LinkedOmics: analyzing multi-omics data within and across 32 cancer types. *Nucleic Acids Res.* *46*, D956–D963. <https://doi.org/10.1093/nar/gkx1090>.
40. Mootha, V.K., Lindgren, C.M., Eriksson, K.F., Subramanian, A., Sihag, S., Lehar, J., Puigserver, P., Carlsson, E., Ridderstråle, M., Laurila, E., et al. (2003). PGC-1 α -responsive genes involved in oxidative phosphorylation are coordinately downregulated in human diabetes. *Nat. Genet.* *34*, 267–273. <https://doi.org/10.1038/ng1180>.
41. Warde-Farley, D., Donaldson, S.L., Comes, O., Zuberi, K., Badrawi, R., Chao, P., Franz, M., Grouios, C., Kazi, F., Lopes, C.T., et al. (2010). The GeneMANIA prediction server: biological network integration for gene prioritization and predicting gene function. *Nucleic Acids Res.* *38*, W214–W220. <https://doi.org/10.1093/nar/gkq537>.
42. Schneider, C.A., Rasband, W.S., and Eliceiri, K.W. (2012). NIH Image to ImageJ: 25 years of image analysis. *Nat. Methods* *9*, 671–675. <https://doi.org/10.1038/nmeth.2089>.
43. Györfy, B. (2021). Survival analysis across the entire transcriptome identifies biomarkers with the highest prognostic power in breast cancer. *Comput. Struct. Biotechnol. J.* *19*, 4101–4109. <https://doi.org/10.1016/j.csbj.2021.07.014>.
44. Jézéquel, P., Campone, M., Gouraud, W., Guerin-Charbonnel, C., Leux, C., Ricolleau, G., and Campion, L. (2012). bc-GenExMiner: an easy-to-use online platform for gene prognostic analyses in breast cancer. *Breast Cancer Res. Treat.* *131*, 765–775. <https://doi.org/10.1007/s10549-011-1457-7>.
45. Subramanian, A., Tamayo, P., Mootha, V.K., Mukherjee, S., Ebert, B.L., Gillette, M.A., Paulovich, A., Pomeroy, S.L., Golub, T.R., Lander, E.S., and Mesirov, J.P. (2005). Gene set enrichment analysis: A knowledge-based approach for interpreting genome-wide expression profiles. *Proc. Natl. Acad. Sci. USA* *102*, 15545–15550. <https://doi.org/10.1073/pnas.0506580102>.
46. Li, T., Fan, J., Wang, B., Traugh, N., Chen, Q., Liu, J.S., Li, B., and Liu, X.S. (2017). TIMER: A Web Server for Comprehensive Analysis of Tumor-Infiltrating Immune Cells. *Cancer Res.* *77*, E108–E110. <https://doi.org/10.1158/0008-5472.Can-17-0307>.

STAR★METHODS

KEY RESOURCES TABLE

REAGENT or RESOURCE	SOURCE	IDENTIFIER
Antibodies		
HRP-conjugated Goat Anti-Mouse IgG(H + L)	Proteintech	Cat# SA00001-1; RRID: AB_2722565
HRP-conjugated Goat Anti-Rabbit IgG(H + L)	Proteintech	Cat# SA00001-2; RRID: AB_2722564
ZNF593 Polyclonal antibody	Proteintech	Cat# 19426-1-AP; RRID: AB_10642948
ZNF593 rabbit pAb	Immunoway	Cat# YN7071; RRID: AB_3668764
GAPDH Polyclonal antibody	Proteintech	Cat# 10494-1-AP; RRID: AB_2263076
Alpha Tubulin Polyclonal antibody	Proteintech	Cat# 11224-1-AP; RRID: AB_2210206
Anti-gamma H2A.X (phospho S139)	Abcam	Cat# ab81299; RRID: AB_1640564
Anti-Rad50	Abcam	Cat# ab124682; RRID: AB_11000808
Biological samples		
Human: breast core biopsies	This study	N/A
Chemicals, peptides, and recombinant proteins		
Propidium iodide	MedChemExpress	HY-D0815
Cisplatin	MedChemExpress	HY-17394
Carboplatin	MedChemExpress	HY-17393
Critical commercial assays		
Lipofectamine 2000	Thermo Fisher Scientific	11668019
RNAiso Plus	Takara	9108
PrimeScript RT reagent Kit	Vazyme	R333
SYBR Premix Ex Taq	Vazyme	Q711
BCA protein assay kit	Takara	T9300A
SuperSignal™ West Pico PLUS	Thermo Fisher Scientific	34580
Cell Counting Kit (CCK-8)	Yeasen	40203ES
Deposited data		
TCGA:BRCA	The Cancer Genome Atlas (TCGA) database	https://portal.gdc.cancer.gov/
GEO: GSE1456	Gene Expression Omnibus (GEO) database	https://www.ncbi.nlm.nih.gov/geo/query/acc.cgi?acc=GSE1456
FUSCC-TNBC	The National Omics Data Encyclopedia (NODE)	http://www.biosino.org/node/project/detail/OEP000155
Experimental models: Cell lines		
MDA-MB-231	Laboratory preservation	N/A
SUM159PT	Laboratory preservation	N/A
Oligonucleotides		
siNC:UUCUCCGAACGUGUCACGUTT	RiboBio	N/A
siZNF593#1: UGGAUACCUCUACCGACA	RiboBio	N/A
siZNF593#2: GGUACUUAUCGAUCCAC	RiboBio	N/A
Primers: see Table S1	Sangon Biotech	N/A
Software and algorithms		
R	The R Project for Statistical Computing	www.r-project.org/
the Human Protein Atlas	website	https://www.proteinatlas.org
Linkedomics	Vasaikar et al. ³⁹	http://www.linkedomics.org/login.php
GSEA software	Mootha et al. ⁴⁰	https://www.gsea-msigdb.org/gsea/index.jsp

(Continued on next page)

Continued

REAGENT or RESOURCE	SOURCE	IDENTIFIER
GeneMANIA	Warde-Farley et al. ⁴¹	http://genemania.org/
TIMER	Li et al.	https://cistrome.shinyapps.io/timer/
ImageJ	Schneider et al. ⁴²	https://imagej.net

EXPERIMENTAL MODEL AND STUDY PARTICIPANT DETAILS

The study was approved by the Ethics Committee of the First Hospital of China Medical University, and informed consent was obtained from each participant. The data analyzed in this study were sourced from the TCGA database, GEO database, and FUSCC-TNBC database. The tissue samples involved were all from female breast cancer patients and were snap-frozen in liquid nitrogen immediately after surgical resection and preserved thereafter. The approval number is AF-SOP-07-1.1-01/2019-13. The experimental cell lines used were breast cancer cells MDA-MB-231 and SUM159PT.

METHOD DETAILS**Datasets**

Gene expression profiles and corresponding clinical data for tumors were retrieved from TCGA, and the GSE1456 dataset was obtained from GEO. The information of normal organizations came from Genotype-Tissue Expression database. Additionally, this article validated the conclusions using the FUSCC-TNBC cohort. At the protein expression level, we used the HPA (<https://www.proteinatlas.org>) to analyze ZNF593 expression in breast cancer tissue and normal breast tissue.

Breast cancer samples

Sixty-six breast cancer samples and eight pairs of breast cancer specimens and adjacent normal tissues were obtained from patients who had not received other antitumor therapy or chemotherapy before surgery and were excluded from patients with other malignancies or recurrent metastases. All patients underwent surgery at the Department of Breast Surgery, the First Hospital of China Medical University and signed informed consent. All patients were diagnosed as primary breast cancer by pathologists and had complete follow-up data. The experimental procedures were conducted in accordance with the principles outlined in the Helsinki Declaration and were approved by the Institutional Ethics Review Board of the First Hospital of China Medical University (Approval number: AF-SOP-07-1.1-01/2019-13).

Differential analysis of ZNF593 expression

We used the "tidyverse" package in R version 4.3.2 for differential analysis of ZNF593 expression, including pan cancer and breast cancer versus adjacent normal tissues. The R package "DESeq2" was employed to identify differential expression genes (DEGs) of ZNF593 with the filter criteria $|\log_2FC| > 0.7$ and a p value < 0.05 .

Survival analysis

KM Plotter⁴³ is an online platform for prognostic analysis of cancer patients, utilizing data from European Genome-Phenome Archive (EGA), GEO, and TCGA. Additionally, we validated the association between ZNF593 and survival in breast cancer patients using the R packages "survival" and "survminer". Log rank tests were performed on the survival analysis of breast cancer patients. We also used the website "integrated center for oncology"⁴⁴ to verify the prognostic analysis of ZNF593 in TNBC.

Functional analysis**Linkedomics**

LinkedOmics³⁹ provides a platform for accessing, analyzing, and comparing multi-omics data within and across tumor types. It presented the top 50 genes positively and negatively correlated with ZNF593 in scatterplots and heatmaps.

Enrichment analyses

GO and KEGG analyses were used to investigate functions that ZNF593 and its related genes may be involved in breast cancer. The R package "GSEA", "GSEABase", "clusterProfiler" were employed to perform these enrichment analyses. Additionally, the GSEA software^{40,45} was utilized to uncover underlying regulatory pathways by dividing the samples into two groups based on ZNF593 expression levels.

GeneMANIA

GeneMANIA⁴¹ is a database used for exploring gene interactions and predicting gene functions, presenting interaction results in the form of network graphs. We utilized this database for PPI analysis of ZNF593.

Immune score and the proportion of 22 kinds of immune cells

Utilizing the R package "estimate", we computed the stromal score, immune score, and ESTIMATE score to assess the influence of ZNF593 on the immune microenvironment of breast cancer. And then we used R package "cibersort" and "corrplot" to analyze the proportion of 22 types of immune cells in breast cancer patients.

TIMER

TIMER⁴⁶ can analyze the correlation between two genes in a particular tumor. In this article, we utilized TIMER to analyze the correlation of ZNF593 with the genes related to the markers of immune cells.

IHC

The breast cancer tissue sections were initially deparaffinized and rehydrated. Following overnight incubation with the primary antibody ZNF593 (YN7071, Immunoway), the secondary antibody and DAB reagent were used for staining the breast cancer tissue sections together. Two pathologists independently evaluated the results of IHC staining for each section. The ZNF593 IHC staining results were determined based on both the percentage of positive immunoreactive areas and staining intensity. The IHC score was calculated based on the intensity of staining (0 = negative, 1 = weak, 2 = moderate, 3 = strong) and the percentage of positive tumor cells stained (0 = negative, 1 ≤ 10%, 2 = 10–50%, 3 ≥ 50%). The final IHC score was determined by multiplying the positive staining score by the staining intensity score. The interpretation of the IHC results was performed independently by two pathologists.

Cell culture

Human breast cancer cell lines (SUM159PT, MDA-MB-231) were preserved in the laboratory. The cells were cultured in Dulbecco's Modified Eagle Medium (DMEM) medium. All cell lines were routinely tested negative for mycoplasma contamination with a mycoplasma assay kit (Yeasen, Shanghai, China) and maintained in a 5% CO₂ humidified environment of 37°C.

siRNA construction and transfection

The siRNA targeting ZNF593 was synthesized and purified by RiboBio (Guangzhou, China). siRNA transfection was performed using Lipofectamine 2000 transfection reagent according to the manufacturer's instructions (Thermo Fisher Scientific, USA).

siNC : UUCUCCGAACGUGUCACGUTT,
siZNF593#1: UGGAUACCUCUACCUGACA,
siZNF593#2: GGUACUUCAUCGAUCCAC.

RNA isolation and quantitative reverse transcription polymerase chain reaction (RT-qPCR)

Total RNA was extracted from the samples using RNAiso Plus reagent (Takara, Japan) following the manufacturer's instructions. The extracted RNA was then reverse transcribed into complementary DNA using the PrimeScript RT reagent Kit (Vazyme, China). RT-qPCR was performed using SYBR Premix Ex Taq (Vazyme, China) on a QuantStudio 6 Flex Real-Time PCR System (Applied Biosystems, USA). The mRNA expression levels of the target genes were determined using the 2^{-ΔΔCT} method and normalized to the expression levels of a reference gene. The sequence of primers we used is listed in [Table S1](#).

Western blotting

For western blotting, cultured cells were washed with phosphate-buffered saline (PBS) and lysed in lysis buffer consisting of 50 mM Tris/HCl (pH 7.5), 0.5% Nonidet P-40 (NP-40), 1 mM ethylene diamine tetraacetic acid (EDTA), 150 mM NaCl, 1 mM dithiothreitol, 0.2 mM phenylmethylsulfonyl fluoride, 10 mM pepstatin A, and 1 mM leupeptin. The protein concentration was determined using a BCA protein assay kit (Takara, Shenyang, China) and equal quantities of protein samples (10–100 mg) were used for western blotting analysis and resolved by SDS-PAGE. The separated proteins were transferred to polyvinylidene difluoride (PVDF) membranes (Merck Millipore, USA). The membranes were incubated with indicated primary antibody followed by an horseradish peroxidase (HRP)-conjugated secondary antibody after blocking the membrane with 5% non-fat milk (Solarbio, Shenyang, China), and then detected by enhanced chemiluminescence detection kit (ThermoFisher, Shenyang, China). The details for antibody used in study were listed in [Table S2](#).

ImageJ

ImageJ⁴² is an image processing software, which we utilize in this article to assist with IHC scoring and to conduct quantitative analysis of the grayscale values for some of the western blot bands.

Cell viability

After cellular digestion, the cells were counted and seeded into 96-well plates at a density of 2 × 10³. Transfection was then performed for a duration of 12 h. Cell viability was determined using the CCK-8 from Yeasen (Shanghai, China), following the manufacturer's protocol. To plot the cell proliferation curve, absorbance values were measured at a wavelength of 450 nm at specified time points.

Transwell migration assays

For the cell migration assays, a specific number of cells (ranging from 4–10 × 10⁴) were suspended in serum-free medium and seeded into the top chambers (FALCON, USA). The lower chambers were filled with medium containing 20% fetal bovine serum. Following incubation for a specified time (usually 12 to 48 h), the cells that migrated through the membrane and reached the lower surface were

fixed using methanol and stained with 0.1% crystal violet. Cotton swabs were used to gently remove cells in upper surface. The numbers of migrated cells were counted in randomly selected microscope fields and averaged to obtain representative results.

Flow cytometry analysis

In the cell cycle analysis, cells were fixed with pre-cooled 70% ethanol overnight and then incubated at 37°C for 30 min with propidium iodide (PI, MedChemExpress, China) staining buffer containing 50 µg/ml PI, 200 µg/ml RNase A, and 0.1% Triton X-100 in PBS. Flow cytometry data were generated using an FC500 MPL flow cytometer (Beckman Coulter, Indianapolis, IN, USA).

QUANTIFICATION AND STATISTICAL ANALYSIS

Statistical analyses were carried out using GraphPad (version 9.4.1), R software (version 4.3.2) and SPSS (version 26.0). Statistical analyses of two groups were calculated using Wilcoxon rank-sum tests, two-tailed Student's *t* tests or two-way ANOVA tests. Correlation coefficients were calculated using the Spearman test. Data was presented as the mean ± standard deviation (SD) from at least three independent experiments. $p < 0.05$ was considered as statistically significant (*, $p < 0.05$; **, $p < 0.01$; ***, $p < 0.001$; ****, $p < 0.0001$; ns, no significance).